

# Density Correlations in Matter Wave Jet Emission of a Driven Condensate

Zhigang Wu<sup>1,2</sup> and Hui Zhai<sup>2,3</sup>

<sup>1</sup>Shenzhen Institute for Quantum Science and Engineering and Department of Physics,  
Southern University of Science and Technology, Shenzhen 518055, China

<sup>2</sup>Institute for Advanced Study, Tsinghua University, Beijing, 100084, China

<sup>3</sup>Collaborative Innovation Center of Quantum Matter, Beijing, 100084, China  
(Dated: August 2, 2022)

Emission of matter wave jets has been recently observed in a Bose-Einstein condensate confined by a cylindrical box potential, induced by a periodically modulated inter-particle interaction (Nature **551**, 356 (2017)). In this letter we apply the time-dependent Bogoliubov theory to study the correlation effect observed in this highly non-equilibrium phenomenon. Without any fitting parameter, our theoretical calculations on the angular density correlations are in excellent quantitative agreement with the experimental measurements. We interpret the angular density correlation of the jets as the Hanbury-Brown-Twiss effect between the excited quasi-particles with different angular momenta, and our theory explains the puzzling observation of the asymmetric density correlations between the jets with the same and opposite momenta. Our theory can also identify the main factors that control the height and width of the peaks in the density correlation function, which can be directly verified in future experiments.

The ability to manipulate the inter-particle interaction is one of the truly unique aspects of cold atomic systems [1]. In particular, the flexibility to precisely control the interaction in a spatially dependent [2–4] or temporally dependent manner [5–9] leads to novel situations in a quantum many-body system beyond the paradigms of the traditional condensed matter physics. The recently observed matter wave jet emissions from the Chicago group [10, 11] is such an example, where a time-periodic modulation of the interaction strength is carried out in an essentially open quantum system.

In this experimental work [10], a Bose-Einstein condensate (BEC) is confined within a shallow cylindrical box potential and the inter-particle interaction strength is modulated sinusoidally in time, with the modulation frequency much larger than the height of the barrier. Modulation of the interaction naturally leads to excitations from the BEC with energies on the order of the modulation frequency, and as such the shallow barrier cannot prevent the excitations from escaping the trap. After some duration of modulation, bursts of narrow streams of atoms with concentrated density are observed leaving the barrier along the radial direction, as illustrated in Fig. 1 (a). Such a phenomenon is termed “matter wave jet emission” by Ref. [10] and, as we shall demonstrate, provides an ideal platform for the study of many-body correlation effect in a highly non-equilibrium setting.

The most conspicuous feature of such jet emissions is the fractured density pattern of the ejected atoms in the azimuthal direction in any single measurement. The angular density of the ejected atoms becomes uniform only after averaging over sufficiently many measurements for a given time-of-flight. The underlying azimuthal density pattern in a single image is reflected by the angular density-density correlation, which is found to exhibit peaks at zero and  $\pi$  angles even after the average. This

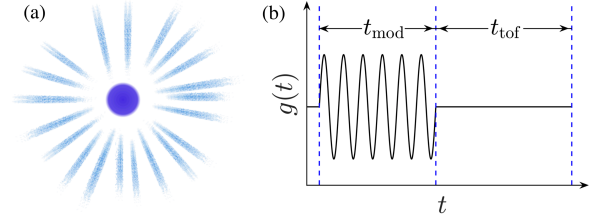


FIG. 1. Illustration of the experimental system in Ref. [10]. (a) Matter wave jets detected from the a disk-shaped BEC with radius  $\rho_0$ . (b) Experimental procedure: the interaction is modulated periodically for a time interval  $t_{\text{mod}}$  and the excited atoms travel radially for another time interval  $t_{\text{tof}}$  before detection.

is reminiscent of the Hanbury-Brown-Twiss (HBT) effect [12–14]. However, Ref. [10] observed a puzzling effect of the correlation, that is the two correlation peaks at zero and  $\pi$  angle are highly asymmetric. Since the bosons are initially condensed in the zero-momentum state, if one naturally assumes that the modulation of the scattering length excites pairs of atoms each carrying opposite momentum, one expects that the two correlation peaks to be symmetric [10]. This observed asymmetry has even drawn attention from high-energy physics community [15] where jet emission phenomenon has been studied extensively in high-energy collisions [16].

In this letter we apply the number-conserving, time-dependent Bogoliubov theory to study the density correlations observed in the jet emissions of the BEC. Without requiring any fitting parameter, we find excellent quantitative agreement between our theory and the experimental observations. A key point of our theory is that we obtain the excitations in the angular momentum bases which respect the symmetry of the geometry of the experimental setup. Thus, our theory can attribute the asymmetry of the density correlation function to the destruc-

tive interferences between atoms with different angular momenta, and can further predict that such destructive interference processes diminish as the time-of-flight  $t_{\text{tof}}$  increases. Furthermore, based on the distribution of excitations in different angular momenta, we are able to reveal how the width of the peak in density correlation depends on the initial condensate size and the driving frequency.

*Time-dependent Bogoliubov theory.* We consider a trapped and weakly-interacting BEC at zero temperature driven from equilibrium by a time-dependent interaction  $g(t)$ . The system is described by the time-dependent Hamiltonian ( $\hbar = 1$  throughout this letter)

$$\hat{H}(t) = \int d\mathbf{r} \hat{\psi}^\dagger(\mathbf{r}) \hat{h} \hat{\psi}(\mathbf{r}) + \frac{g(t)}{2} \int d\mathbf{r} \hat{\psi}^\dagger(\mathbf{r}) \hat{\psi}^\dagger(\mathbf{r}) \hat{\psi}(\mathbf{r}) \hat{\psi}(\mathbf{r}),$$

where  $\hat{h}(\mathbf{r}) = -\frac{\nabla^2}{2m} + V_{\text{tr}}(\mathbf{r})$  is the single particle Hamiltonian with  $m$  being the atom mass and  $V_{\text{tr}}(\mathbf{r})$  the trapping potential. The dynamics of the system for  $t > 0$  can be investigated by means of the time-dependent Bogoliubov theory. In this framework, we consider the time-evolution of the Heisenberg field operator  $\hat{\psi}_H(\mathbf{r}, t) = \Phi_0(\mathbf{r}, t) + \delta\hat{\psi}_H(\mathbf{r}, t)$ , where  $\Phi_0(\mathbf{r}, t)$  is the time-dependent condensate wave function and  $\delta\hat{\psi}_H(\mathbf{r}, t)$  is the fluctuation operator. The latter is determined by the Bogoliubov transformation  $\delta\hat{\psi}_H(\mathbf{r}, t) = \sum_j [u_j(\mathbf{r}, t) \hat{\beta}_j - v_j^*(\mathbf{r}, t) \hat{\beta}_j^\dagger]$ , where  $\hat{\beta}_j^\dagger, \hat{\beta}_j$  are the quasi-particle operators for the initial equilibrium Hamiltonian at  $t = 0$ . The time-dependent Bogoliubov amplitudes  $u_j, v_j$  can be calculated from the coupled Bogoliubov-de Gennes (BdG) equations [17, 18]

$$\begin{aligned} i\partial_t u_j(\mathbf{r}, t) &= \hat{\mathcal{L}}(\mathbf{r}, t) u_j(\mathbf{r}, t) - g(t) \Phi_0^*(\mathbf{r}, t) v_j(\mathbf{r}, t) \\ i\partial_t v_j(\mathbf{r}, t) &= -\hat{\mathcal{L}}(\mathbf{r}, t) v_j(\mathbf{r}, t) + g(t) \Phi_0^*(\mathbf{r}, t) u_j(\mathbf{r}, t), \end{aligned} \quad (1)$$

where  $\hat{\mathcal{L}}(\mathbf{r}, t) \equiv \hat{h}(\mathbf{r}) + 2g(t)|\Phi_0(\mathbf{r}, t)|^2 - \mu$  with  $\mu$  as the initial chemical potential of the BEC. Generally, the BdG equations in Eq. (1) should be solved in conjunction with a time-dependent Gross-Pitaevskii (GP) equation determining the condensate wave function  $\Phi_0(\mathbf{r}, t)$ , subjected to the constraint of particle number conservation

$$N = \int d\mathbf{r} \left( |\Phi_0(\mathbf{r}, t)|^2 + \left\langle \delta\hat{\psi}_H^\dagger(\mathbf{r}, t) \delta\hat{\psi}_H(\mathbf{r}, t) \right\rangle \right). \quad (2)$$

Once the Bogoliubov amplitudes are determined, all relevant physical quantities can be readily calculated.

We now apply the theory outlined above to study the experiment in Ref. [10]. There the BEC is trapped by a potential which can be modelled by  $V_{\text{tr}}(\mathbf{r}) = V_{\text{tr}}(\rho, \theta, z) = V_h \Theta(\rho - \rho_0) + m\omega_z^2 z^2/2$ , where  $\Theta(x)$  is the Heaviside step function,  $\rho_0$  and  $V_h$  are respectively the radius and the height of the cylindrical barrier and  $\omega_z$  is the trapping frequency in the vertical direction. At time  $t > 0$ , the atomic scattering length is subjected to a sinusoidal oscillation with the frequency  $\Omega \gg V_h$  for a duration of  $t_{\text{mod}}$  and is then held at the background value

for another duration  $t_{\text{tof}}$  for the time-of-flight, that is,  $g(t) = 4\pi[a_{\text{bg}} + a_{\text{am}} \sin(\Omega t) \Theta(t_{\text{mod}} - t)]/m$  (see Fig. 1). Here  $a_{\text{bg}}$  is the background scattering length and  $a_{\text{am}}$  is the amplitude of the oscillation. Before solving the BdG equations, we make two observations which will simplify our calculations:

i) Since the background interaction between the atoms is extremely weak with  $a_{\text{bg}} = 5a_0$  and the vertical trapping is relatively strong with  $\omega_z = 2\pi \times 210$  Hz, we find that that number of excitations to higher harmonic oscillator states of the vertical trap is negligible during the dynamic process. Thus, in the following calculations we shall consider that all atoms stay in the lowest single-particle eigenstate  $\varphi_0(z)$  of the vertical harmonic trap. This is also consistent with the experimental fact that the measured root-mean-square radius of the condensate is in excellent agreement with the harmonic oscillator length along the vertical direction. Furthermore, due to the box trapping potential in the 2D plane, the condensate density is always uniform within the cylindrical barrier and quickly vanishes beyond the radius of the barrier. Thus the time-dependent condensate wave function can be well approximated by  $\Phi_0(\mathbf{r}, t) \approx \sqrt{n_0(t)} \varphi_0(z) \Theta(\rho_0 - \rho)$ , which renders solving the GP equation unnecessary.

ii) The cylindrical-shaped trap makes it most appropriate to choose the angular momentum eigenstates as the basis to solve the BdG equations. More specifically we consider as the basis the eigenstates  $\chi_{lk}(\mathbf{r}) = \varphi_0(z) e^{il\theta} \phi_{lk}(\rho) / \sqrt{2\pi}$  of the single particle Hamiltonian  $\hat{h}(\mathbf{r})$  with eigenenergy  $\epsilon_{lk}$ , where  $l$  is the angular momentum quantum number,  $k$  labels the radial modes of  $\hat{h}(\mathbf{r})$  and  $\phi_{lk}(\rho)$  is the radial wave function. Due to the angular momentum conservation, we can label the Bogoliubov amplitudes by the index  $j \equiv (l, q)$ , where  $q$  labels the radial modes of the initial equilibrium BdG equations. Thus we can write

$$u_{lq}(\mathbf{r}, t) = \sum_k \chi_{lk}(\mathbf{r}) U_{kq}^{(l)}(t); \quad v_{lq}(\mathbf{r}, t) = \sum_k \chi_{lk}(\mathbf{r}) V_{kq}^{(l)}(t).$$

Using the above expansion, the BdG equations in Eq. (1) are then converted into two first order differential equations for the matrices  $U^{(l)}$  and  $V^{(l)}$ , which can be solved under the constraint in Eq. (2).

In the following calculations, all the parameters, including the initial atom number, interaction strengths, trap parameters and the time durations, are chosen to be exactly the same as those used in the experiment.

*Angular Mode Distribution.* First, we consider the mode distribution for the excited atoms. The total number of atoms excited after a modulation time  $t_{\text{mod}}$  is

$$N_{\text{ex}} = \left\langle \delta\hat{\psi}_H^\dagger(\mathbf{r}, t_{\text{mod}}) \delta\hat{\psi}_H(\mathbf{r}, t_{\text{mod}}) \right\rangle = \sum_l N_l, \quad (3)$$

where  $N_l = \sum_q \int d\mathbf{r} |v_{lq}(\mathbf{r}, t_{\text{mod}})|^2$  is the number of atoms excited to states with angular momentum  $l$ . For a sufficiently long modulation time, modes with a range of

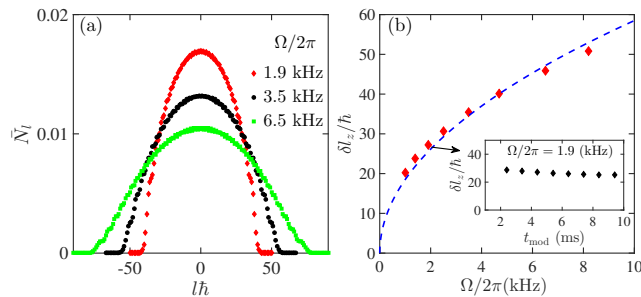


FIG. 2. (a) The fraction of atoms  $\bar{N}_l$  with angular momentum  $l\hbar$  for three different driving frequencies at  $t_{\text{mod}} = 4.4$  ms. (b) The angular momentum fluctuation per atom  $\delta l_z$  as a function of the driving frequency at  $t_{\text{mod}} = 4.4$  ms. The inset shows  $\delta l_z$  as a function of  $t_{\text{mod}}$  for  $\Omega = 2\pi \times 1.9$  kHz. The dashed line is a fit by the function  $\alpha\rho_0\sqrt{\Omega}$ . Unless specified otherwise, the following parameters are the same for all the calculations: the atom number  $N = 30000$ , the condensate radius  $\rho_0 = 8.5$   $\mu\text{m}$  and the modulation amplitude  $a_{\text{am}} = 60a_0$ .

angular momenta can be significantly occupied. This is shown in Fig. 2 (a), where the fraction of excited atoms with angular momentum  $l$ ,  $\bar{N}_l \equiv N_l/N_{\text{ex}}$ , is plotted for several modulation frequencies with an experimental  $t_{\text{mod}} = 4.4$  ms. For all the occupied radial modes with the same angular momentum, a sharp resonance is found at the energy  $\sim \Omega/2$ . Physically, the resonance at  $\Omega/2$  results from the fact that pairs of atoms with opposite angular momentum are excited due to the angular momentum conservation, splitting the total energy quanta  $\Omega$  absorbed by the condensate.

Now, the energy of an out-going excited atom can be divided into a rotational part and a radial kinetic part, which together yield  $\Omega/2$  at resonance. The radial kinetic energy decreases as the angular momentum increases, and the occupation of an angular momentum state vanishes when the rotational energy saturates  $\Omega/2$ . In other words, the rotational energy of an atom with angular momentum  $l$  is  $\sim l^2/m\rho_0^2 \leq \Omega/2$ . Thus the occupation in angular momentum states has a cut-off  $l_c$  which determines the width of the distribution and is proportional to  $\rho_0\sqrt{\Omega}$ . A more precise characterisation of the width of the angular momentum distribution is the angular momentum fluctuation per particle  $\delta l_z = \sqrt{\sum_l l^2 \bar{N}_l}/N_{\text{ex}}$ , which is shown in Fig. 2 (b) for various driving frequencies employed in the experiments. We expect that  $\delta l_z$  is proportional to the cut-off  $l_c$  and, as shown in Fig. 2 (b), it is indeed well described by the function  $\alpha\rho_0\sqrt{\Omega}$ , where  $\alpha$  is a constant. Furthermore, we find that after some initial transient period  $\delta l_z$  depends neither on the modulation time nor on the time-of-flight. As we can see from the inset of Fig. 2 (b),  $\delta l_z$  shows little change for  $t_{\text{mod}}$  ranging from 2 ms to 10 ms. During the time-of-flight,  $\delta l_z$  remains unchanged because no more atoms are excited. As we shall see later, this fact determines the robustness of zero correlation peak in the dynamical

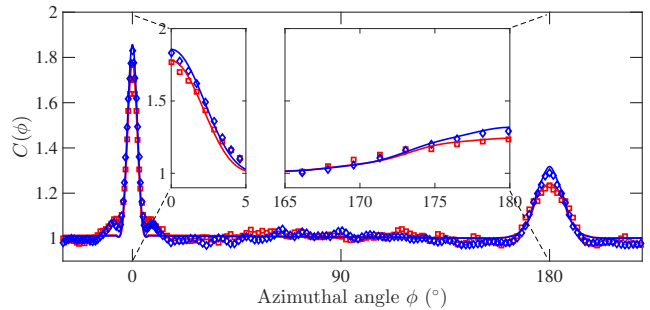


FIG. 3.  $C(\phi, t)$  calculated with  $t_{\text{mod}} = 4.4$  ms (red) and 5.6 ms (blue) for  $\Omega = 2\pi \times 1.9$  kHz and  $t = 36$  ms. The experimental measurements are all taken at  $t = t_{\text{mod}} + t_{\text{tof}} = 36$  ms [19] and are shown in symbols in corresponding colors. The insets are expanded views of the correlation peaks.

process of jet emission.

*Angular Density Correlation.* We now consider the angular density correlation function defined as

$$C(\phi, t) = \frac{2\pi \int d\theta \langle \delta \hat{n}_H(\theta, t) \delta \hat{n}_H(\theta + \phi, t) \rangle}{\langle \int d\theta \delta \hat{n}_H(\theta, t) \rangle^2}, \quad (4)$$

where  $\delta \hat{n}_H(\theta, t) \equiv \int dz \int d\rho \rho \delta \hat{\psi}_H^\dagger(\mathbf{r}, t) \delta \hat{\psi}_H(\mathbf{r}, t)$ . Using the Bogoliubov transformation and expressing the Bogoliubov amplitudes as  $u_{lq}(\mathbf{r}) = \varphi_0(z) e^{il\theta} \tilde{u}_{lq}(\rho)/\sqrt{2\pi}$  and  $v_{lq}(\mathbf{r}) = \varphi_0(z) e^{il\theta} \tilde{v}_{lq}(\rho)/\sqrt{2\pi}$ , we obtain

$$C(\phi, t) = 1 + \sum_{l'l'} C_{ll'}(t) e^{i(l+l')\phi}, \quad (5)$$

where  $C_{ll'}(t) = N_{\text{ex}}^{-2} \sum_{qq'} [G_{lq, l'q'} + G_{l'q', lq}] G_{lq, l'q'}^*$  with  $G_{lq, l'q'}(t) = \int d\rho \rho \tilde{u}_{lq}(\rho, t) \tilde{v}_{l'q'}(\rho, t)$ . If we consider situations where the excited atoms have travelled away from the condensate, the expression in Eq. (5) suggests that the experiments are essentially measuring a HBT type correlation between atoms in different angular momentum states. In Fig. 3, we compare the correlation function calculated from Eq. (5) for two different modulation times to those measured in experiment. The agreement between our theory and the experiment is remarkable, considering that the jet emission is a highly non-equilibrium process. A noteworthy property of the correlation function is the asymmetrical distribution between peaks at  $\phi = 0$  and at  $\phi = \pi$ , which is accurately captured by our theory. This asymmetry can in fact be clearly seen from Eq. (5), where all the terms inside the summation contribute constructively for  $\phi = 0$  while the terms with odd  $l + l'$  contribute destructively to the correlation peak at  $\pi$  leading to a reduction of its height. This is in contrast to the theory in Ref. [10], which uses the plane wave bases and assumes the conservation of momentum in pair production. Consequently, it always leads to a symmetric distribution between 0 and  $\pi$ . In fact, due to the finite size and the disk geometry of the condensate, the momentum conservation is not a good assumption as far as the correlation is concerned.

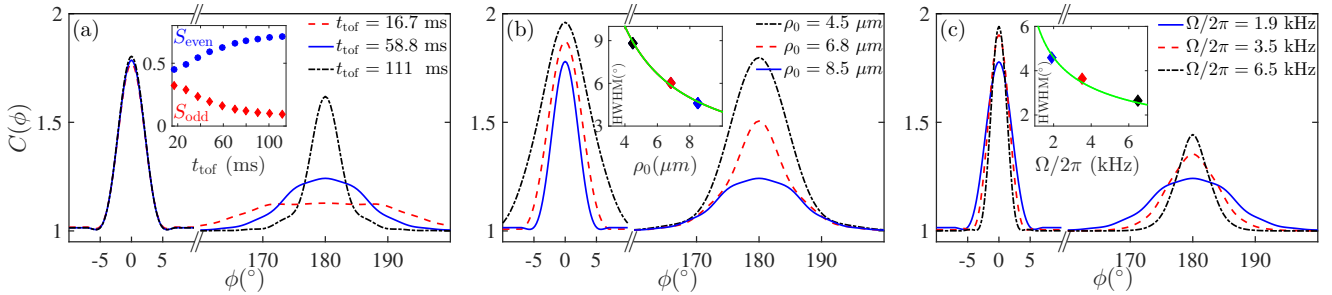


FIG. 4. (a)  $C(\phi)$  calculated for different  $t_{\text{tof}}$  with the same  $t_{\text{mod}} = 4.4$  ms. The inset shows the behaviour of  $S_{\text{even}}$  and  $S_{\text{odd}}$  during time-of-flight (see text). (b)  $C(\phi)$  calculated for condensates of different radius (same density as that in (a)) with  $t_{\text{mod}} = 4.4$  ms and  $t_{\text{tof}} = 31.6$  ms. The inset shows that the half-width at half-maximum (HWHM) of the zero peak as a function of  $\rho_0$  behaves as  $\sim 1/\rho_0$  (green line). The driving frequency for both (a) and (b) is  $\Omega = 2\pi \times 1.9$  kHz. (c)  $C(\phi)$  calculated for different driving frequencies. The inset shows that the HWHM of the zero peak as a function of  $\Omega$  behaves as  $\sim 1/\sqrt{\Omega}$  (green line).

In addition to making comparisons to the experiments, our theory can also reveal systematically how the density correlation depends on the time-of-flight  $t_{\text{tof}}$ , the initial condensate radius  $\rho_0$  and the driven frequency  $\Omega$ . For  $t_{\text{tof}}$ , as shown in Fig. 4 (a), the density correlation function is calculated for three increasingly longer  $t_{\text{tof}}$  with the modulation time fixed at  $t_{\text{mod}} = 4.4$  ms. We see that on the one hand the zero peak remains almost identical during the time-of-flight, and on the other the  $\pi$  peak begins with a plateau structure at small  $t_{\text{tof}}$ , becomes progressively sharper as  $t_{\text{tof}}$  increases and eventually becomes similar to the zero peak.

The robustness of the zero peak during the time-of-flight can be understood from the Heisenberg uncertainty principle that  $\delta\phi\delta l_z \sim \hbar$ . As demonstrated earlier, the angular momentum fluctuation per atom  $\delta l_z \sim \alpha\rho_0\sqrt{\Omega}$  depends weakly on  $t_{\text{mod}}$  or  $t_{\text{tof}}$ , which explains a time-insensitive of the peak at zero angle. This also leads to the conclusion that the zero peak width is proportional to  $1/\rho_0$  and  $1/\sqrt{\Omega}$ . This is confirmed by numerical calculation presented in Fig. 4 (b) and (c). In Fig. 4 (b), we increase the radius of the condensate  $\rho_0$  while keeping all other parameters fixed and we find that the width of the zero peak indeed decreases as  $1/\rho_0$ . Similarly in Fig. 4 (c), we vary the driving frequency  $\Omega$  alone and find that the width of the zero peak decreases as  $1/\sqrt{\Omega}$ . All these results are consistent with the uncertainty principle.

We turn next to the time evolution of the  $\pi$  peak shown in Fig. 4 (a). As shown in the inset of Fig. 4 (a), we find that the destructive contribution  $S_{\text{odd}} = \sum_{l+l'=\text{odd}} C_{ll'}(t)$  gradually decreases toward zero as  $t_{\text{tof}}$  increases and the asymmetry eventually disappears. Meanwhile,  $S_{\text{even}} = \sum_{l+l'=\text{even}} C_{ll'}(t)$  grows such that the peak at  $\phi = 0$  stay almost unchanged. For measurements performed at a sufficiently long  $t_{\text{tof}}$ , the asymmetry disappears because the ejected atoms are in the far field where the condensate can be essentially viewed as a point source. Thus all the atoms emanating from this point source would have perfect symmetry with respect

to the origin of the ejection. In other words, the relative size of the condensate from the perspective of the ejected atoms at the time of detection plays a crucial role in the asymmetry of the correlation function. This is also confirmed by results shown in Fig. 4 (b) and (c). We see in Fig. 4 (b) that for the same  $t_{\text{tof}}$  and driving frequency  $\Omega$ , the two peaks become increasingly more symmetrical when the condensate radius decreases. In Fig. 4 (c), we see that the  $\pi$  peak also becomes sharper as the driving frequency increases, even though the  $t_{\text{tof}}$  is held the same. This is because a higher driving frequency translates into a larger escape velocity for the ejected atoms and thus a larger distance from the condensate for the same  $t_{\text{tof}}$ . The situation then is similar to that in Fig. 4 (a) where the asymmetry in the correlation diminishes as the ejected atoms move further away from the condensate.

*Ejected Atoms.* Finally, as a demonstration that the capacity of our theory is not limited to the study of the correlation function, we calculate the number of ejected atoms and compare with the experimental measurements. For a sufficiently long  $t_{\text{tof}}$ , all the excited atoms will eventually leave the barrier after the modula-

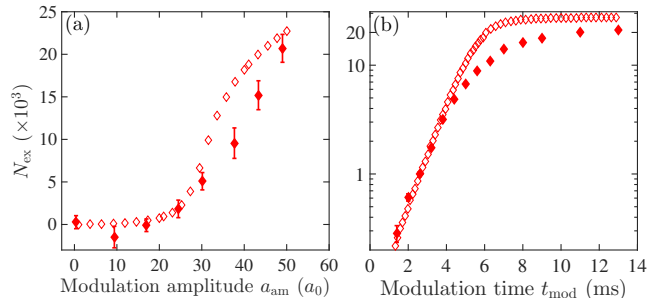


FIG. 5. (a): The number of excited atoms as a function of  $a_{\text{am}}$  for  $\Omega = 2\pi \times 4500$  Hz and  $t_{\text{mod}} = 25$  ms. (b): The number of excited atoms (logarithmic scale) as a function of  $t_{\text{mod}}$  for  $a_{\text{am}} = 60a_0$  and  $\Omega = 2\pi \times 1900$  Hz. The filled symbols are the experimental measurements.

tion stops at  $t_{\text{mod}}$ . Thus, the number of ejected atoms detected at time  $t = t_{\text{mod}} + t_{\text{tof}}$  simply equals to the number of excited atoms  $N_{\text{ex}}(t)$  at  $t = t_{\text{mod}}$ . In Fig. 5, we show  $N_{\text{ex}}(t_{\text{mod}})$  calculated from Eq. (3) both as a function of  $a_{\text{am}}$  for a fixed  $t_{\text{mod}}$  and as a function of  $t_{\text{mod}}$  for a fixed  $a_{\text{am}}$ . Without any fitting parameter, the overall agreements between our calculations and the experimental measurements are again excellent.

*Conclusion.* We interpret the angular density correlation observed in the jet emission as the HBT effect of quasi-particles in different angular momenta, excited by a periodical modulation of the interaction of a cylindrically trapped Bose condensate. The average density distribution is uniform along the azimuthal direction since there is no coherence between quasi-particles with different angular momenta. The density-density correlation, however, can exhibit interferences manifested as the HBT effect, and the asymmetry between zero and  $\pi$  peaks are due to the difference between the constructive and destructive interferences. Because of the perfect agreement between theory and experiment without any fitting parameter, our theoretical framework can be applied to study future experiments in this and similar settings.

*Acknowledgement.* This work is supported by China Postdoctoral Science Foundation under Grant No. 2017M620034 (ZW), MOST under Grant No. 2016YFA0301600 (HZ) and NSFC Grant No. 11734010 (HZ). We thank C. Chin, J. Midtgaard, L. Feng, L. Clark for very helpful discussions. We also want to thank the Chicago group for providing the measurement data presented in Ref. [10].

- 
- [1] C. Chin, R. Grimm, P. Julienne, and E. Tiesinga, *Rev. Mod. Phys.* **82**, 1225 (2010).
  - [2] R. Yamazaki, S. Taie, S. Sugawa, and Y. Takahashi, *Phys. Rev. Lett.* **105**, 050405 (2010).
  - [3] M. Yan, B. J. DeSalvo, B. Ramachandhran, H. Pu, and T. C. Killian, *Phys. Rev. Lett.* **110**, 123201 (2013).
  - [4] L. W. Clark, L.-C. Ha, C.-Y. Xu, and C. Chin, *Phys. Rev. Lett.* **115**, 155301 (2015).
  - [5] S. Jochim, M. Bartenstein, A. Altmeyer, G. Hendl, S. Riedl, C. Chin, J. Hecker Denschlag, and R. Grimm, *Science* **302**, 2101 (2003).
  - [6] P. Engels, C. Atherton, and M. A. Hoefer, *Phys. Rev. Lett.* **98**, 095301 (2007).
  - [7] S. E. Pollack, D. Dries, R. G. Hulet, K. M. F. Magalhães, E. A. L. Henn, E. R. F. Ramos, M. A. Caracanhas, and V. S. Bagnato, *Phys. Rev. A* **81**, 053627 (2010).
  - [8] V. I. Yukalov, A. N. Novikov, and V. S. Bagnato, *Laser Physics Letters* **11**, 095501 (2014).
  - [9] M. C. Tsatsos, J. H. V. Nguyen, A. U. J. Lode, G. D. Telles, D. Luo, V. S. Bagnato, and R. G. Hulet, *arXiv:1707.04055*.
  - [10] L. W. Clark, A. Gaj, L. Feng, and C. Chin, *Nature* **551**, 356 EP (2017).
  - [11] L. Feng, J. Hu, L. W. Clark, and C. Chin, *arXiv:1803.01786*.
  - [12] R. H. Brown and R. Q. Twiss, *Nature* **177**, 27 EP (1956).
  - [13] S. Fölling, F. Gerbier, A. Widera, O. Mandel, T. Gericke, and I. Bloch, *Nature* **434**, 481 EP (2005).
  - [14] M. Schellekens, R. Hoppeler, A. Perrin, J. V. Gomes, D. Boiron, A. Aspect, and C. I. Westbrook, *Science* **310**, 648 (2005).
  - [15] M. Arratia, *arXiv:1801.05515*.
  - [16] R. Feynman, R. D. Field, and G. C. Fox, *Nucl. Phys. B* **128**, 1 (1977).
  - [17] Y. Castin and R. Dum, *Phys. Rev. Lett.* **79**, 3553 (1997).
  - [18] Y. Castin and R. Dum, *Phys. Rev. A* **57**, 3008 (1998).
  - [19] L. W. Clark, private communication.